different immunoglobulin subclasses reacted to the sections simultaneously overnight at 4°C. The sections were incubated with 2 Alexa Fluor–conjugated secondary antibodies for relevant immunoglobulin subclasses. For multicolor staining, we always obtained images by sequentially scanning with each laser line to avoid the fluorescence bleeding. The sections were evaluated by 2 investigators.

In Situ Tetramer Staining

HTLV-1 Tax–specific T lymphocytes were detected with either phycoerythrin (PE)-labeled HLA-A*0201/Tax11-19-tetramer or HLA-A*2402/Tax301-309-tetramer (MBL, Japan) diluted to 1.0 μg/mL. HLA-A*0201/Tax11-19-pentamer was also used to corroborate the results of the tetramer in the staining of the CNS. Phycoerythrin-labeled HLA-A*0201/HIV Gag peptide (SLYNTVATL) tetramer or PE-labeled HLA-A*2402/HIV Env peptide (RYLKDQQLL) tetramer was used as an irrelevant control. The sections were fixed with PBS-buffered 0.1% PFA for 10 minutes and washed with PBS after each step. The sections were incubated with tetramer overnight at 4°C in the presence of proteinase inhibitors (Roche, Tokyo, Japan) and subsequently fixed again with PBS-buffered 4% PFA for 20 minutes at RT. Rabbit anti-PE Ab (500×; BioGenesis, Westminister, CO) was used as the secondary Ab and incubated with the sections for 60 minutes at RT. The signal was enhanced with the EnVision+ system and visualized with AEC chromogen. For immunofluorescence staining, the sections were incubated with goat anti-rabbit Ab labeled with Alexa Fluor 488 for 60 minutes at RT. For double staining, sections were simultaneously incubated with any of anti-CD8 mAb, anti–granzyme B mAb, anti–interferon-γ (IFN-γ) mAb, or Lt-4 mAb and with Tax-tetramer. After overnight incubation and fixation, the sections were incubated with rabbit anti-PE Ab for 60 minutes. The sections were then incubated with Alexa Fluor 594–conjugated anti–mouse IgG1 or IgG3 Ab and Alexa Fluor 488–conjugated goat anti-rabbit IgG Ab for 60 minutes at RT. 4′,6-Diamidino-2-phenylindole was used for counterstaining. To determine the frequency of Tax-tetramer–positive cells among the CD8-positive cells, we counted the cells under full-field observation (400×).

Detection of HTLV-1–Infected Cells in the Tissues

Fresh-frozen spinal cord sections were used to detect HTLV-1 proteins. The sections were dried and fixed with 4% PFA for 20 minutes at RT. Anti–HTLV-1 Tax mAb (Lt-4), anti–HTLV-1 Gag mAb (TP-7), or anti–HTLV-1 Env mAb (65/6C2) was applied to the sections in combination with anti-CD3 mAb, anti-CD4 mAb, or anti–Ki-67 Ab. After the sections were incubated overnight at 4°C, they were incubated with isotype-specific secondary antibodies for 60 minutes at RT in the dark and subsequently counterstained with DAPI.

Detection of Apoptotic Cells

Apoptotic cells were detected with anti–active caspase-3 Ab or anti–single-stranded DNA Ab by light microscopy and confocal laser scanning microscopy. The cells were also detected with TdT-mediated dUTP nick end labeling method according to the manufacturer's instructions (ApopTag Millipore, Billerica, MA).

RESULTS

General Findings in the CNS of HAM/TSP Patients

Transverse sections of the spinal cords of HAM/TSP patients demonstrated atrophy in the lateral columns with thickened meninges (Fig. 1A–C). Symmetric patchy myelin pallor in Luxol fast blue staining was observed in the affected long tracts, lateral cerebrospinal fasciculus, ventral and dorsal spinocerebellar fasciculi, spinothalamic fasciculus in the lateral column, and fasciculus gracilis in the posterior columns. The essential histopathologic feature was a chronic progressive inflammatory process with marked parenchymal exudation of lymphocytes and macrophages around the vessels (i.e. postcapillary venules) in both the gray and white matter of the spinal cord (Fig. 1D, E). The degree of cellular infiltration was strong in Patients 6315 and 8624, whereas Patient 6664 had no significant cell infiltrates (Table 1). Neurons in the anterior horns were generally preserved (Fig. 1F). Immunohistochemical staining of the spinal cord revealed remarkable infiltration of CD8-positive cells (Fig. 1G, H) and CD4-positive cells (Fig. 1I) and macrophages (data not shown) throughout the parenchyma, especially in perivascular areas. These histochemical findings are consistent with previous reports.

Detection of HTLV-1 Tax–Specific CTLs in the CNS

To validate the in situ tetramer staining procedure for visualization of HTLV-1–specific CTLs, PBMCs of HLA-A*02–positive patients with HAM/TSP were fixed on slides and stained with HLA-A*02/Tax11-19 tetramer and anti-CD8 mAb. The fluorescence pattern of the tetramer exactly colocalized with that of anti-CD8 mAb on the PBMCs (Fig. 2A). This is consistent with the fact that CD8 cells express a T-cell

FIGURE 1. Routine and histochemical study of spinal cords from patients with HTLV-1–associated myelopathy/tropical spastic paraparesis (HAM/TSP) by light microscopy. **(A–C)** The spinal cord (**A**, cervical level; **B**, lower thoracic level; **C**, lumbar level) of a HAM/TSP patient shows marked atrophy in the lateral columns; original magnification is 40×. The bars indicate 3 mm. **(A)** Symmetric myelin pallor is noted in the lateral cerebrospinal fasciculus, ventral and dorsal spinocerebellar fasciculus, lateral spinothalamic fasciculus in the lateral column (arrowhead), anterior spinothalamic fasciculus in the anterior column (thick arrow), and fasciculus gracilis in the posterior column (thin arrow). **(B)** There is marked atrophy, particularly of the lateral column. **(C)** Mild atrophy in the lumbar level. **(D)** A number of infiltrating cells are scattered throughout the section of the spinal cord. **(E)** Perivascular and parenchymal mononuclear cell infiltrates. **(F)** Neurons in the anterior horn are fairly preserved in the atrophied spinal cord. **(G, H)** Immunohistochemical study revealed that markedly infiltrating CD8-positive cells (red) are scattered in the parenchyma and around a small vessel in the spinal cord. **(I)** CD4-positive cells (red) are observed around a small vessel in the spinal cord. Nuclei were counterstained with hematoxylin (**D–I**, blue). Scale bar = 100 μm. **(A–C)** Luxol fast blue; **(D–F)** hematoxylin and eosin; **(G–I)** immunohistochemistry with hematoxylin counterstain.

receptor. We could not detect HTLV-1–specific CTLs at all with Tax-tetramer or -pentamer in frozen samples using a reported procedure for nonfrozen samples (20). We tested several modified staining procedures and finally found that prefixing the frozen sections at a very low concentration of PFA was optimal. We selected the sections that stained best with the tetramer or pentamer from several sections from each block. We detected HTLV-1 Tax11-19–specific CTLs in the parenchyma of the spinal cords from an HLA-A*02–positive patient (Fig. 2B) and an HLA-A*24–positive patient (Fig. 2C) with HLA-A*02/Tax-tetramer and HLA-A*24/Tax-tetramer, respectively. The CTLs were also detected in the thickened leptomeninges (Fig. 2D). On the other hand, no cells were detected by HIV Gag-tetramer and influenza-tetramer as tetramer controls (Fig. 2E).

Accumulation of HTLV-1 Tax–Specific CD8-positive CTLs in the CNS

To determine the frequency of HTLV-1 Tax–specific CTLs in CD8-positive lymphocytes infiltrating the CNS, we performed double staining for HTLV-1 Tax–specific CTLs and CD8-positive lymphocytes. Tax-specific CTLs stained with Tax-tetramer were frequently noted in the lesions. Double staining revealed that the fluorescence of Tax-tetramer colocalized with that of anti-CD8 mAb in all 3 patients (Fig. 3A–C). Meanwhile, HIV-tetramer restricted by either HLA-A*02 or HLA-A*24 did not bind any CD8-positive cells in the corresponding specimen (Fig. 3D). Next, we evaluated the frequency of Tax-specific CTLs in CD8-positive lymphocytes in 4 sections of the spinal cord from each patient. The percentages of Tax-specific CTLs in CD8-positive cells were 22.1% (62 of 280) and 31.1% (96 of 309) in patients with HLA-A*02–positive and HLA-A*24–positive patients, respectively (Table 3). Patient 6664 had no significant cellular infiltrates, and we only detected 2 HLA-A*24/Tax-tetramer–positive and no HLA-A*02/Tax-tetramer–positive cells in the 4 sections of the spinal cord from that patient. In addition to Tax-tetramer, Tax-pentamer was also used for the staining of the tissues from Patient 8624 to corroborate our results with Tax-tetramer. Similarly, the fluorescence of Tax-pentamer exactly colocalized with that of anti-CD8 mAb; the frequency of Tax-pentamer–positive cells in CD8-positive cells was 31% in the lesion (Fig. 3E).

Detection of HTLV-1 Proteins in the CNS

Although the HTLV-1 gene has been detected in CD4-positive lymphocytes, its viral protein has not been detected in freshly isolated lymphocytes. Therefore, we used HTLV-1–infected cell lines in a preliminary study for visualizing HTLV-1 Tax protein. Detected HTLV-1 Tax showed a patchy staining pattern in the nuclei of a human cell line (Figure, Supplemental Digital Content 1, parts A and B, http://links.lww.com/NEN/A676). Although HTLV-1 Tax was not detected in noncultured PBMCs, we detected the protein in PBMCs of patients with HAM/TSP after 8-hour culture (Figure, Supplemental Digital Content 1, part C, http://links.lww.com/NEN/A676).

We next detected 3 HTLV-1 proteins (Tax, Env, and Gag) in the CNS tissues of the HAM-TSP patients. Tax was found in the cells near vessels (Fig. 4A, B) and in the leptomeninges. The nuclear protein Tax showed a patchy staining pattern in the nuclei (Fig. 4C, D, G), whereas Env and Gag were detected in the cell membrane or cytoplasm (Fig. 4E–G). Double staining revealed that the cells expressing Tax, Env, or Gag were CD4-positive lymphocytes (Fig. 4C–F). CD68-, CD8-, CNPase-, and glial fibrillary acidic protein (GFAP)–positive cells were not positive for HTLV-1 Tax (Figure, Supplemental Digital Content 2, http://links.lww.com/NEN/A677). To investigate whether HTLV-1–infected cells proliferate in the CNS, we stained with anti-Tax mAb and anti–Ki-67 Ab (a marker of cell proliferation); however, Ki-67–positive Tax-positive cells were very rare; we detected only 2 cells in the 2 sections (data not shown). To investigate the frequency of HTLV-1–infected cells in the CD4-positive population and the frequency of apoptotic cells in HTLV-1–infected cells, we performed triple staining for CD4, active caspase-3, and HTLV-1 Env protein. The HTLV-1–positive cells in infiltrating CD4-positive cells were 60.3% and 82.4% in Patients 8624 and 6315, respectively (Table 3). More than 50% of infiltrating CD4-positive cells were infected with HTLV-1. Furthermore, HTLV-1–infected cells had a greater tendency to undergo apoptosis than noninfected cells; 36.4% of the infected cells were undergoing apoptosis, whereas 10.3% of noninfected cells were undergoing apoptosis in Patient 8624 (Table 3). Because the sample from Patient 6664 showed only a few cellular infiltrates, we could not evaluate the frequency of apoptosis in that case.

Functional Molecules of HTLV-1–Specific CD8-Positive CTLs

To investigate whether HTLV-1 Tax–specific CD8-positive CTLs have the ability to attack HTLV-1–infected CD4-positive cells in the CNS, we attempted to detect functional molecules of CTLs in the CNS. Granzyme B–, perforin-, and IFN-γ–positive cells were detected in both parenchymal and perivascular areas (Fig. 5A–C). Some of the cells stained with Tax-tetramer were positive for granzyme B (Fig. 5D). Furthermore, double staining revealed that CD8-positive cells sometimes were in contact with HTLV-1–infected cells (Fig. 5E), and that some HTLV-1 Tax–specific CTLs were next to HTLV-1–infected cells in the parenchyma (Fig. 5F). Human T-lymphotropic virus type-1 Tax–specific CTLs were not positive for Ki-67 (data not shown).

Apoptotic Cells

Next, we determined which cells underwent apoptosis in the CNS of the patients. Active caspase-3–positive cells (apoptotic cells) were frequently observed near CD8-positive cells in the parenchyma of the spinal cord, and some of them were in contact with CD8-positive cells (Fig. 5G–I). Active caspase-3 showed granular staining patterns in our pictures, although it has shown a diffuse cytoplasmic pattern in previous studies. The staining pattern may differ because of the different conditions of the frozen samples. We tried to detect the apoptotic cells with formalin-fixed paraffin-embedded samples by light microscopy. Caspase-3 was detected in the cell cytoplasm in those samples (Fig. 6A). Next, we stained the sections by methods other than the anti–active caspase-3 Ab to corroborate

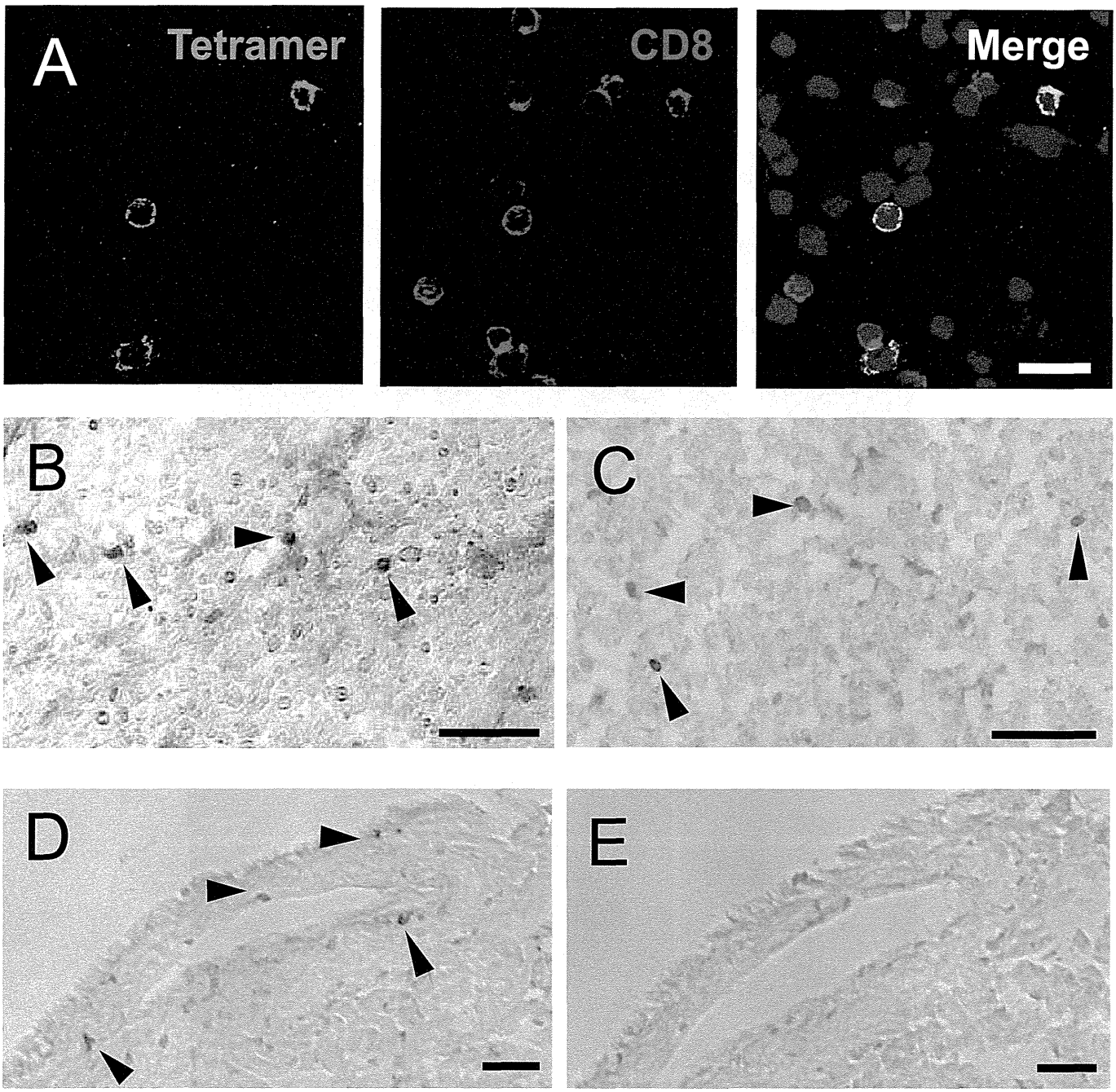

FIGURE 2. Detection of CD8-positive human T-lymphotropic virus type-1 (HTLV-1) Tax–specific cytotoxic T lymphocytes (CTLs) in peripheral blood mononuclear cells (PBMCs) and CNS. **(A)** Double staining with anti-CD8 monoclonal antibody (red) and HLA-A*0201/Tax11-19 or HLA-A*2402/Tax11-19 tetramer (green) was performed with confocal laser scanning microscopy (CLSM). DAPI (blue) was used for counterstaining the nuclei. The 3 colors were captured sequentially using CLSM. Merged images are shown on the right. PBMCs from a patient with HAM/TSP are stained with the tetramer. **(B)** HLA-A*0201/Tax11-19-tetramer–positive cells are scattered in the spinal cord parenchyma (Patient 8624). **(C)** HLA-A*2402/Tax301-309-tetramer–positive cells are seen in the parenchyma of the spinal cord (Patient 6315). **(D)** Cells stained with HLA-A*0201/Tax11-19-tetramer are found around the vessel in the spinal cord leptomeninges (Patient 8624) (red). **(E)** No cells are stained with HLA-A*0201/HIV Gag-tetramer in the adjacent serial section. White and black bars indicate 20 μm and 100 μm, respectively.

the frequent apoptosis in the spinal cord. Using a TdT-mediated dUTP nick end labeling assay, we detected a number of apoptotic cells (Fig. 6B, C). We also stained these spinal cord samples with anti–single-stranded DNA Ab and obtained similar findings (Fig. 6E). Altogether, the 3 staining methods showed frequent apoptosis in the affected spinal cords (Fig. 6).

Double staining revealed that apoptotic cells were CD4-positive or CD68-positive cells (Fig. 7D, E). Interestingly,

oligodendrocytes, which were stained with anti-CNPase mAb (Fig. 7B), were frequently undergoing apoptosis (Fig. 7F). This finding is consistent with the occurrence of demyelination in the spinal cords of HAM/TSP patients. However, oligodendrocytes were not stained with anti–HTLV-1 Tax mAb (data not shown) or anti–HLA-ABC Ab (Fig. 7G). Astrocytes that were stained with anti-GFAP mAb were diffusely distributed throughout the parenchyma (Fig. 7A), whereas GFAP-positive cells

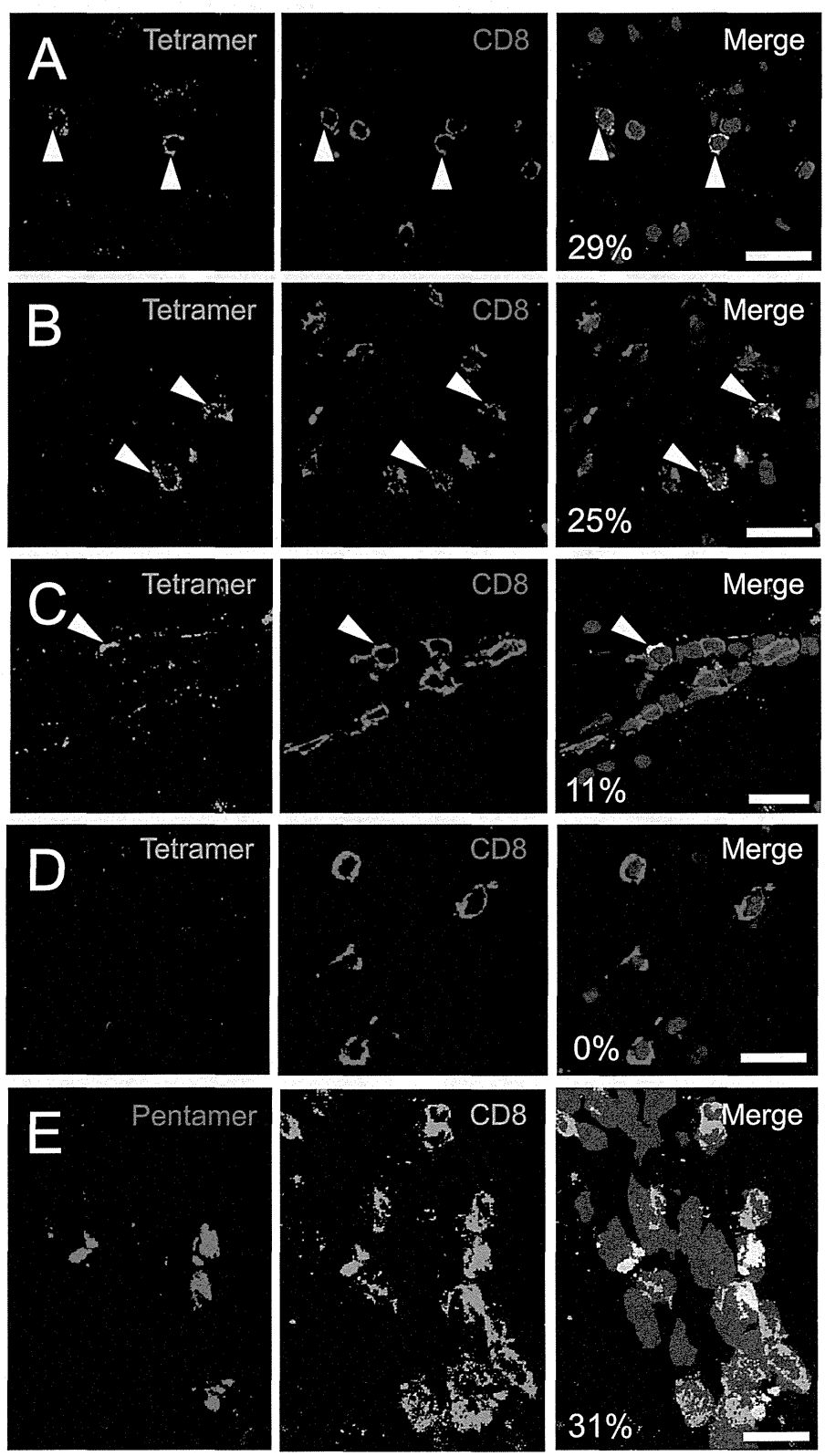

TABLE 3. Cytotoxic T Lymphocytes, Human T-Lymphotrophic Virus-1–Infected Cells and Apoptotic Cells in the CNS

Patient ID	Tax-Specific CTLs in CD8-Positive Cells	Env-Positive Cells in CD4-Positive Cells	Caspase-3–Positive Cells in CD4-Positive Cells	Caspase-3–Positive Cells in Env-Positive CD4-Positive Cells	Caspase-3–Positive Cells in Env-Negative CD4-Positive Cells
8624	22.1% (62/280)*	60.3% (44/73)	26.0% (19/73)	36.4% (16/44)	10.3% (3/29)
6315	31.1% (96/309)	82.4% (103/125)	12.0% (15/125)	12.6% (13/103)	9.1% (2/22)
6664	N/A†	N/A	N/A	N/A	N/A

*The numbers of positive cells/total cells are indicated within parentheses.
†Not applicable; cell infiltration was not significant for evaluation.
CTL, cytotoxic T lymphocytes.

were not positive for active caspase-3 (Fig. 7H). Neurons identified by their size as well as several particles within the neuronal body induced strong autofluorescence but were not positive for active caspase-3 (data not shown).

DISCUSSION

One of the most striking features of the cellular immune responses in patients with HAM/TSP is the highly increased numbers of HTLV-1–specific CTLs in PBMCs and CSF (14, 15); however, little is known about CTLs in the CNS. The fixation of human CNS samples with a very low concentration of PFA made it possible to visualize antigen-specific CTLs using tetramers or a pentamer in the CNS. Strikingly, their frequency reached more than 20% in CD8-positive cells that had migrated to the CNS. In a flow cytometric study in our cohort, we detected HTLV-1 Tax11-19–specific and HTLV-1 Tax301-309–specific CTLs in PBMCs from patients with HAM/TSP at 2.25% (0.0%–18.7%) (26) and 4.34% (0.2%–17.6%) (unpublished data), respectively. The present data are consistent with another report in which the frequency of HTLV-1 Tax–specific CTLs was higher in CSF than in PBMCs (18). Although the frequency of the CTLs differs by the case, it may be attributed to the difference in the phase of the disease or the duration of the illness.

Granzyme B and perforin, both known as cytotoxic molecules of CTLs, were detected along with IFN-γ in the parenchyma near the vessels in the CNS. Some CTLs contained granzyme B. Human T-lymphotropic virus type-1–specific CTLs were in contact with HTLV-1–infected cells, and apoptotic cells were frequently noted near the CD8-positive cells. These results strongly suggest that the infiltrating CTLs function as effector cells in the CNS. Interestingly, a considerable number of oligodendrocytes underwent apoptosis in the affected lesions. Meanwhile, the oligodendrocytes neither increase the expression levels of HLA-ABC nor express HTLV-1 proteins. The HTLV-1–positive cells were only infiltrating CD4-positive T cells. These results suggest that HTLV-1–infected CD4-positive T cells, but not oligodendrocytes, are the main targets of HTLV-1–specific CTLs in the CNS, and that an interaction between these infected CD4-positive cells and CTLs may cause bystander damage in oligodendrocytes that is associated with demyelination. Similarly, in a previous study on an animal model of neurotropic mouse coronavirus infection, activated CD8-positive T cells specific to neither the virus nor CNS antigens caused demyelination (27). Mechanisms of demyelination in other viral infections in the CNS, even those exhibiting dense infiltration of activated CTLs such as measles or lymphocytic choriomeningitis virus encephalitis, are unclear. Whereas a CD8-positive CTL has been considered to be beneficial for the host infected by a certain virus by diminishing virus-infected cells, recent studies clearly show that strong CTL responses to a pathogen sometimes induce an immunopathology that is harmful to the host. For example, in a mouse model of CNS lymphocytic choriomeningitis virus infection, the depletion of CD8-positive T cells rescues the animal from a fatal condition (28). In another report, highly activated CD8-positive T cells in the brain were correlated with early CNS dysfunction in simian immunodeficiency virus infection (29). Similarly, markedly increased HTLV-1–specific CTLs in the CNS may induce the development of HAM/TSP.

Previous studies reported that the HTLV-1 antigen is hardly detected in PBMCs (30, 31), despite a high proviral

FIGURE 3. Frequency of human T-lymphotropic virus type-1 (HTLV-1)-1 Tax–specific cytotoxic T lymphocytes (CTLs) in CD8-positive lymphocytes. Double staining with anti-CD8 monoclonal antibody (mAb) (red) and HLA-A*0201/Tax11-19 or HLA-A*2402/Tax301-309 tetramer (green) was performed with confocal laser scanning microscopy (CLSM). DAPI (blue) was used for counterstaining the nuclei. The 3 colors were captured sequentially using CLSM. Merged images are shown in the right-hand column. **(A–C)** Spinal cords from the 3 patients with HAM/TSP were stained with the tetramers. CTLs stained with the tetramer were exclusively positive for CD8. The arrowheads indicate CTLs. **(A)** Double staining with HLA-A*0201/Tax11-19 tetramer and anti-CD8 mAb (Patient 8624). HTLV-1–specific CTLs are observed in the parenchyma and comprise 29% of CD8-positive cells in the field. **(B)** Double staining with HLA-A*2402/Tax301-309 tetramer and anti-CD8 mAb (Patient 6315). The CTLs comprise 25% of CD8-positive cells in the field. **(C)** Double staining with HLA-A*2402/Tax301-309 tetramer and anti-CD8 mAb (Patient 6664). CTLs are visible in the perivascular area and comprise 11% (1 of 9) of CD8-positive cells in the field. **(D)** Double staining with HLA-A*2402/HIV Gag tetramer (tetramer control) and CD8 in Patient 6315. No cells are stained with the tetramer. **(E)** To corroborate the staining with the tetramer, an HLA pentamer was used for double staining (Patient 8624). Similarly, fluorescence of the HLA-A*02/Tax11-19 pentamer (red in left-hand column) is exclusively colocalized with that of CD8 (green in middle column), as shown by yellow in the merged image (right-hand column) in the thickened meninges. The percentage of Tax pentamer–positive cells in CD8-positive cells is 31% (5 of 16) of the CD8-positive cells in the field. White bars indicate 20 μm.

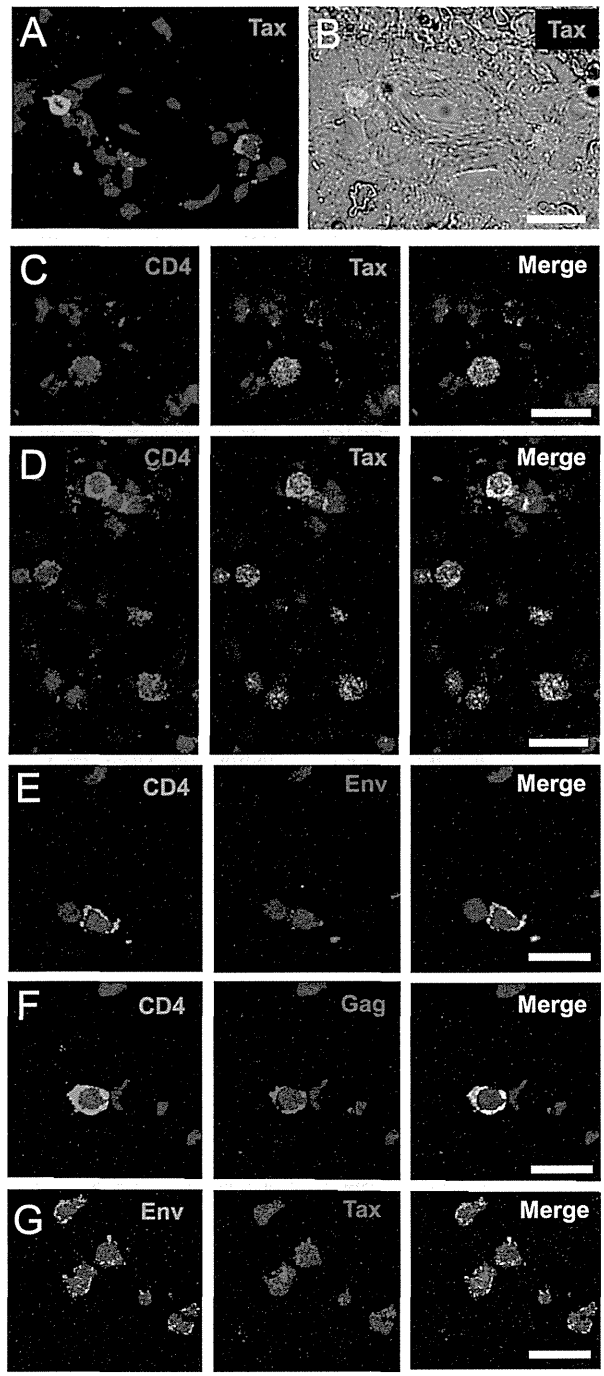

FIGURE 4. Detection of CD4-positive human T-lymphotropic virus type-1 (HTLV-1)–infected cells in CNS parenchyma. **(A, B)** Cells expressing HTLV-1 Tax protein were found near the vessels of the spinal cord of Patient 6315. **(C, D)** Double staining for CD4 (purple) and HTLV-1 Tax (green) revealed that visualized HTLV-1 Tax showed a patchy staining pattern in the nuclei in parenchyma **(C)** and in meninges **(D)**. **(E)** Double staining for CD4 (green) and HTLV-1 Env protein (red) revealed that HTLV-1 Env is costained with CD4 on the cell surface. **(F)** Double staining for CD4 (green) and HTLV-1 Gag protein (red) revealed that HTLV-1 Gag is detected in the cytoplasm of CD4-positive cells. **(G)** Double staining for HTLV-1 Env (green) and HTLV-1 Tax (red) revealed that both proteins were detected separately in the same cells. The nuclei were counterstained with DAPI. White bars indicate 20 μm.

load (12). We also failed to detect any HTLV-1 proteins by the immunohistochemical or flow cytometric study in PBMCs from 20 HAM/TSP patients, even though the proteins became detectable after short-term culturing (Figure, Supplemental Digital Content 1, part C, http://links.lww.com/NEN/A676). Although the evidence of both vigorous persistent CTLs immune responses and increased IgM antibody specific for HTLV-1 in the peripheral blood of HAM/TSP patients have suggested that

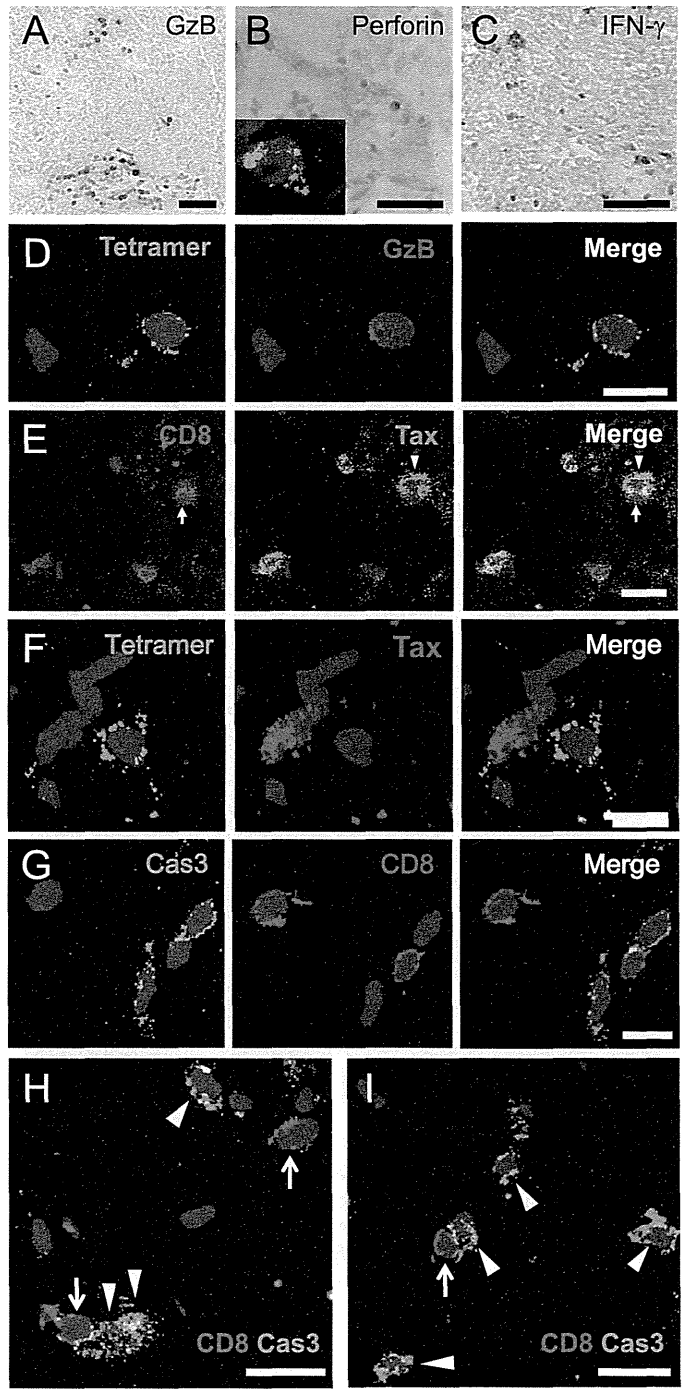

FIGURE 5. Cytotoxic T-lymphocyte (CTL) molecules in the CNS. **(A–C)** Immunohistochemistry shows granzyme B (GzB)–positive cells **(A)**, perforin-positive cells **(B)**, and interferon-γ (IFN-γ)–positive cells **(C)** in the perivascular area of the spinal cord of Patient 8624. Black bars indicate 100 μm. **(D)** Double staining with HLA-A*2402/Tax301-309-tetramer (green) and anti–granzyme B monoclonal antibody (mAb) (red) reveals a GzB-positive HTLV-1–specific CTL in the parenchyma of the spinal cord (Patient 6315). **(E)** A cell expressing HTLV-1 Tax protein is in contact with a CD8-positive cell in the spinal cord of Patient 6315. **(F)** An HTLV-1 Tax–specific CTL is next to the cell expressing Tax protein in the spinal cord of Patient 8614. **(G–I)** Double staining for active caspase-3 (Cas3) (green) and CD8 (red, arrows in **[H]** and **[I]**) reveals CD8-positive cells in contact with active caspase-3–positive cells in the spinal cord of Patient 8624. Nuclei were counterstained with DAPI. White bars indicate 10 μm.

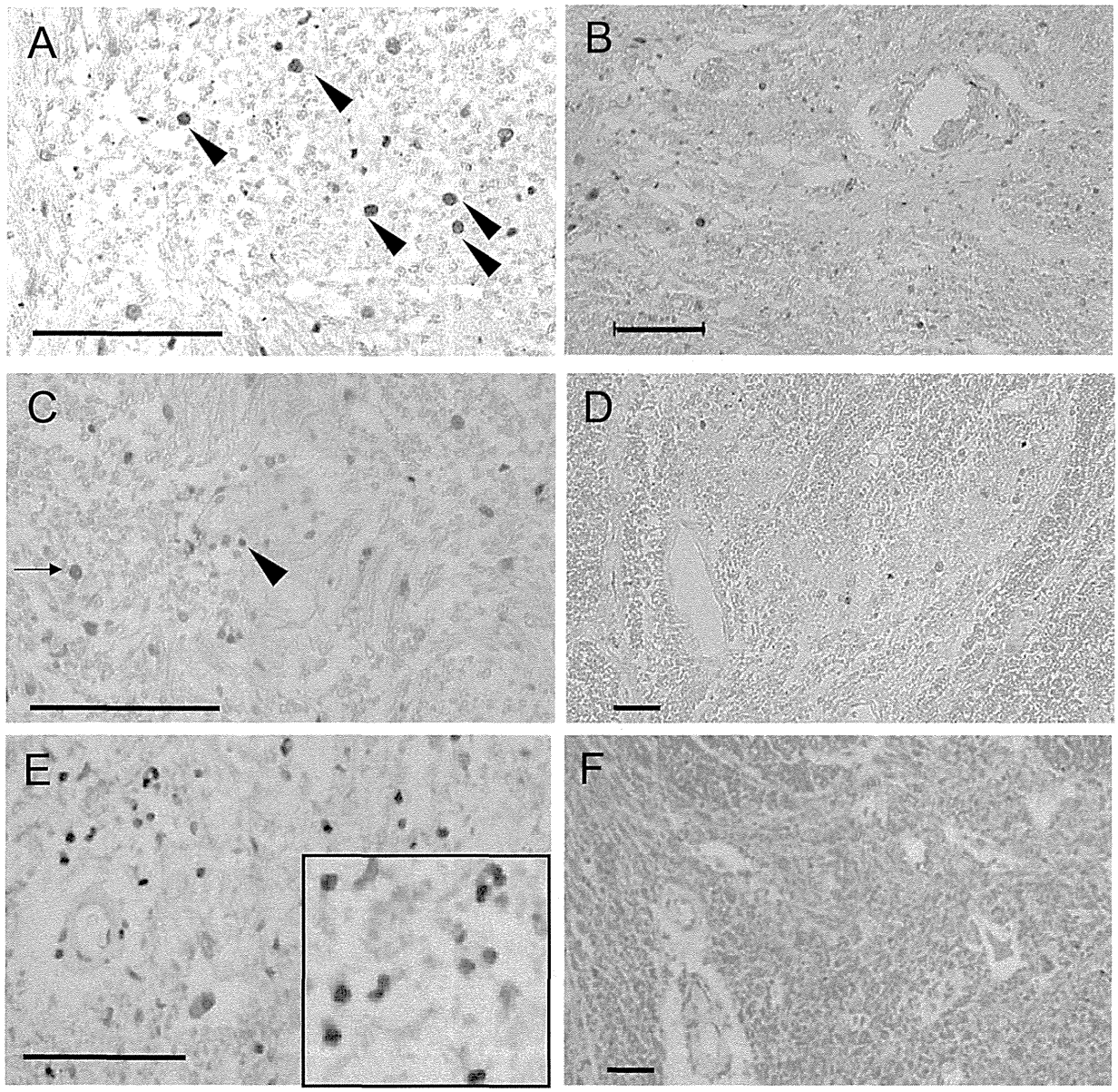

FIGURE 6. Detection of apoptotic cells in the CNS. **(A)** Some small cells are apoptotic (DAB; brown, arrowheads) detected by anti–active caspase-3 antibody (Ab). **(B–D)** TdT-mediated dUTP nick end labeling assay. **(B)** A number of apoptotic cells (DAB; brown) are detected in the spinal cord of a patient with HTLV-1–associated myelopathy/tropical spastic paraparesis (Patient 8624). **(C)** Some infiltrating small cells around a small vessel (arrowhead) and some relatively large cells in the parenchyma (arrow) are apoptotic. **(D)** The apoptotic cells are barely detectable in the control spinal cord from an HTLV-1–seronegative patient with hepatoma. **(E, F)** Anti-single-stranded DNA antibody staining. **(E)** Numerous apoptotic cells (AEC; red) are detected in the spinal cord (Patient 8624). A higher magnification picture in the inset shows apoptotic cells. **(F)** Apoptotic cells are barely detectable in the control patient spinal cord. Scale bar = 100 μm.

HTLV-1–infected cells could express viral antigens anywhere in the body of the infected individuals (14, 32), the expression of HTLV-1 proteins in vivo has remained elusive so far.

In this study, we succeeded in detecting HTLV-1 proteins in the CD4-positive T cells infiltrating the CNS. This is consistent with our previous reports in which HTLV-1–infected cells were determined to be CD4-positive lymphocytes in the CNS by in situ hybridization for HTLV-1 mRNA and in situ polymerase chain reaction for HTLV-1 DNA (33, 34). The infiltrating HTLV-1–infected CD4-positive cells may easily express the viral antigens in the CNS, which in turn facilitates the accumulation of HTLV-1–specific CTLs.

Human T-lymphotropic virus type-1 infection causes several organ-specific inflammatory diseases including HAM/TSP (2, 3). Previous reports demonstrating that HTLV-1 proviral loads are high in affected organs such as the muscles, lungs, and CNS suggest that HTLV-1–infected cells accumulate in the organs (13, 35). The pathogenesis model in which both

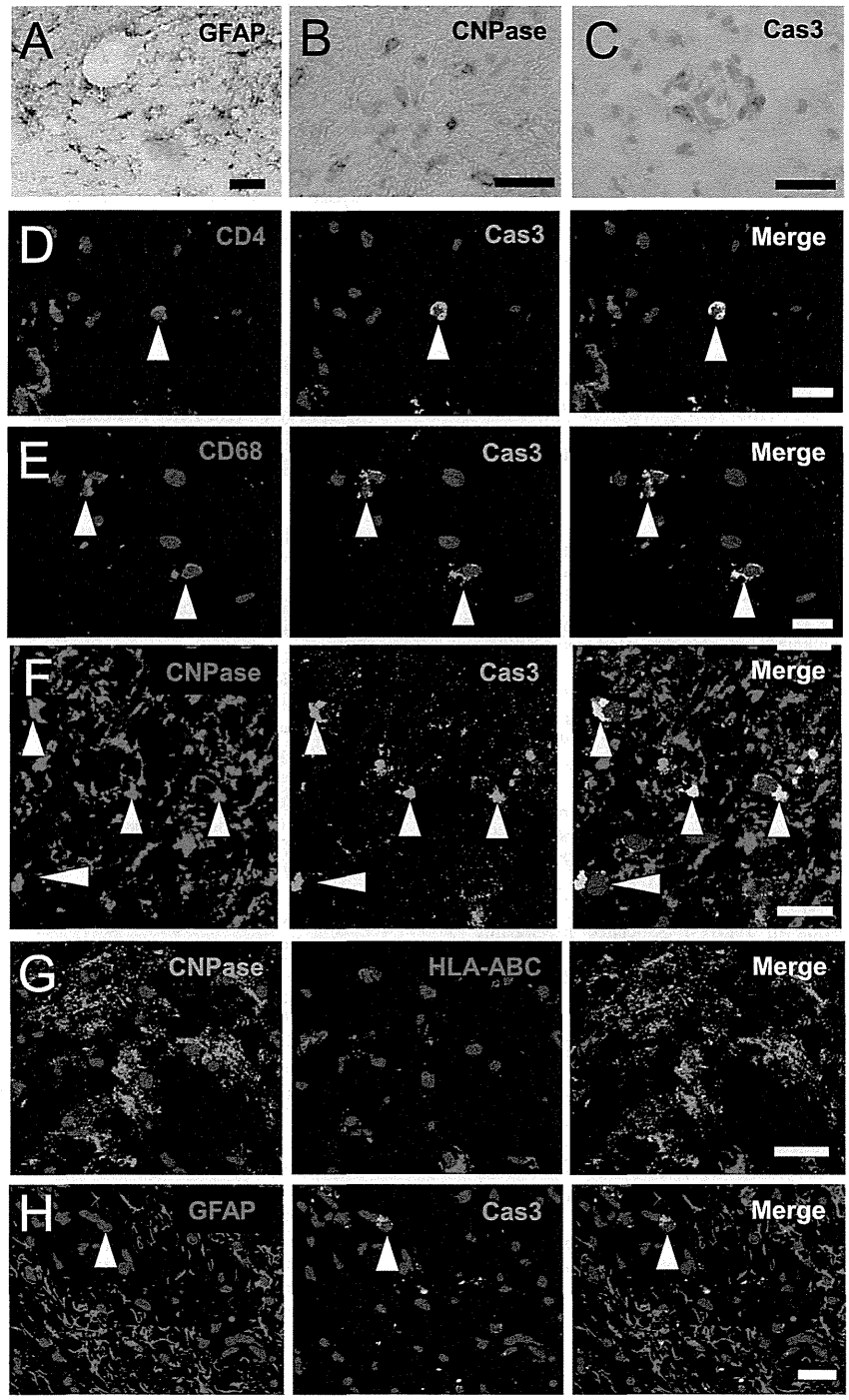

FIGURE 7. Cell identification of apoptotic cells. **(A–C)** Astrocytes **(A)**, oligodendrocytes **(B)**, and apoptotic cells **(C)** were stained with anti–glial fibrillary acidic protein (GFAP) antibody (Ab), anti–2′,3′-cyclic-nucleotide 3′-phosphodiesterase (CNPase) monoclonal antibody (mAb), or anti–active caspase-3 Ab, respectively, in the spinal cord of Patient 8624. Nuclei were counterstained with hematoxylin. **(D–F, H)** Double staining revealed that a CD4-positive cell (red, **D**), a CD68-positive cell (red, **E**), and some oligodendrocytes (red, **F**), but no astrocytes (red, **H**), were apoptotic (green) (arrowheads) in the spinal cord of Patient 8624. **(G)** Double staining with anti-CNPase mAb (green) and anti–HLA-ABC mAb (red) revealed that no oligodendrocyte expresses HLA-ABC. There is no double-positive signal (yellow) in the merged image. White bars indicate 20 μm. Cas3, active caspase-3.

HTLV-1–infected CD4-positive T cells and the virus-specific CD8-positive CTLs infiltrate the organs from the peripheral blood followed by bystander tissue damage may explain why HTLV-1 infection can cause several chronic inflammatory diseases in various organs. Further studies are needed to determine whether the similar immunopathologic model can be applied to HTLV-1–associated inflammatory diseases in other organs.

ACKNOWLEDGMENT

The authors thank Ms. T. Inoue for her excellent technical assistance.

REFERENCES

1. Uchiyama T, Yodoi J, Sagawa K, et al. Adult T-cell leukemia: Clinical and hematologic features of 16 cases. Blood 1977;50:481–92
2. Gessain A, Barin F, Vernant JC, et al. Antibodies to human T-lymphotropic virus type-I in patients with tropical spastic paraparesis. Lancet 1985;2: 407–10
3. Osame M, Usuku K, Izumo S, et al. HTLV-I–associated myelopathy: A new clinical entity. Lancet 1986;1:1031–32
4. Osame M, Matsumoto M, Usuku K, et al. Chronic progressive myelopathy associated with elevated antibodies to human T-lymphotropic virus type I and adult T-cell leukemialike cells. Ann Neurol 1987;21:117–22
5. Nakao K, Ohba N, Isashiki M, et al. Pigmentary retinal degeneration in patients with HTLV-I–associated myelopathy. Jap J Ophthalmol 1989; 33:383–91
6. Nishioka K, Maruyama I, Sato K, et al. Chronic inflammatory arthropathy associated with HTLV-I. Lancet 1989;1:441
7. Morgan OS, Rodgers-Johnson P, Mora C, et al. HTLV-1 and polymyositis in Jamaica. Lancet 1989;2:1184–87
8. Higuchi I, Nerenberg M, Yoshimine K, et al. Failure to detect HTLV-I by in situ hybridization in the biopsied muscles of viral carriers with polymyositis. Muscle Nerve 1992;15:43–47
9. Ozden S, Gessain A, Gout O, et al. Sporadic inclusion body myositis in a patient with human T cell leukemia virus type 1–associated myelopathy. Clin Infect Dis 2001;32:510–14
10. Matsuura E, Umehara F, Nose H, et al. Inclusion body myositis associated with human T-lymphotropic virus–type I infection: Eleven patients from an endemic area in Japan. J Neuropathol Exp Neurol 2008;67:41–49
11. Sugimoto M, Nakashima H, Watanabe S, et al. T-lymphocyte alveolitis in HTLV-I–associated myelopathy. Lancet 1987;2:1220
12. Nagai M, Usuku K, Matsumoto W, et al. Analysis of HTLV-I proviral load in 202 HAM/TSP patients and 243 asymptomatic HTLV-I carriers: High proviral load strongly predisposes to HAM/TSP. J Neurovirol 1998;4:586–93
13. Hayashi D, Kubota R, Takenouchi N, et al. Accumulation of human T-lymphotropic virus type I (HTLV-I)–infected cells in the cerebrospinal fluid during the exacerbation of HTLV-I–associated myelopathy. J Neurovirol 2008;14:459–63
14. Jacobson S, Gupta A, Mattson D, et al. Immunological studies in tropical spastic paraparesis. Ann Neurol 1990;27:149–56
15. Kubota R, Furukawa Y, Izumo S, et al. Degenerate specificity of HTLV-1–specific $CD8^+$ T cells during viral replication in patients with HTLV-1–associated myelopathy (HAM/TSP). Blood 2003;101:3074–81
16. Biddison WE, Kubota R, Kawanishi T, et al. Human T cell leukemia virus type I (HTLV-I)–specific $CD8^+$ CTL clones from patients with HTLV-I–associated neurologic disease secrete proinflammatory cytokines, chemokines, and matrix metalloproteinase. J Immunol 1997;159:2018–25
17. Kubota R, Kawanishi T, Matsubara H, et al. Demonstration of human T lymphotropic virus type I (HTLV-I) tax–specific $CD8^+$ lymphocytes directly in peripheral blood of HTLV-I–associated myelopathy/tropical spastic paraparesis patients by intracellular cytokine detection. J Immunol 1998;161:482–88
18. Greten TF, Slansky JE, Kubota R, et al. Direct visualization of antigen-specific T cells: HTLV-1 Tax11-19–specific CD8(+) T cells are activated in peripheral blood and accumulate in cerebrospinal fluid from HAM/TSP patients. Proc Natl Acad Sci USA 1998;95:7568–73
19. Levin MC, Lehky TJ, Flerlage AN, et al. Immunologic analysis of a spinal cord-biopsy specimen from a patient with human T-cell lymphotropic virus type I–associated neurologic disease. N Engl J Med 1997;336:839–45
20. Skinner PJ, Daniels MA, Schmidt CS, et al. Cutting edge: In situ tetramer staining of antigen-specific T cells in tissues. J Immunol 2000; 165:613–17
21. Ijichi S, Izumo S, Eiraku N, et al. An autoaggressive process against bystander tissues in HTLV-I–infected individuals: A possible pathomechanism of HAM/TSP. Med Hypoth 1993;41:542–47
22. Kozako T, Arima N, Toji S, et al. Reduced frequency, diversity, and function of human T cell leukemia virus type 1–specific $CD8^+$ T cell in adult T cell leukemia patients. J Immunol 2006;177:5718–26
23. Yashiki S, Fujiyoshi T, Arima N, et al. HLA-A*26, HLA-B*4002, HLA-B*4006, and HLA-B*4801 alleles predispose to adult T cell leukemia: The limited recognition of HTLV type 1 tax peptide anchor motifs and epitopes to generate anti-HTLV type 1 tax CD8(+) cytotoxic T lymphocytes. AIDS Res Hum Retroviruses 2001;17:1047–61
24. Bunce M, O'Neill CM, Barnardo MC, et al. Phototyping: Comprehensive DNA typing for HLA-A, B, C, DRB1, DRB3, DRB4, DRB5 & DQB1 by PCR with 144 primer mixes utilizing sequence-specific primers (PCR-SSP). Tissue Antigens 1995;46:355–67
25. Lee B, Tanaka Y, Tozawa H. Monoclonal antibody defining tax protein of human T-cell leukemia virus type-I. Tohoku J Exp Med 1989;157:1–11
26. Hayashi D, Kubota R, Takenouchi N, et al. Reduced Foxp3 expression with increased cytomegalovirus-specific CTL in HTLV-I–associated myelopathy. J Neuroimmunol 2008;200:115–24
27. Haring JS, Pewe LL, Perlman S. Bystander CD8 T cell–mediated demyelination after viral infection of the central nervous system. J Immunol 2002;169:1550–55
28. Fung-Leung WP, Kundig TM, Zinkernagel RM, et al. Immune response against lymphocytic choriomeningitis virus infection in mice without CD8 expression. J Exp Med 1991;174:1425–29
29. Marcondes MC, Burudi EM, Huitron-Resendiz S, et al. Highly activated CD8(+) T cells in the brain correlate with early central nervous system dysfunction in simian immunodeficiency virus infection. J Immunol 2001;167:5429–38
30. Kannagi M, Matsushita S, Shida H, et al. Cytotoxic T cell response and expression of the target antigen in HTLV-I infection. Leukemia 1994; 1(Suppl 8):S54–59
31. Hanon E, Asquith RE, Taylor GP, et al. High frequency of viral protein expression in human T cell lymphotropic virus type 1–infected peripheral blood mononuclear cells. AIDS Res Hum Retroviruses 2000; 16:1711–15
32. Nagasato K, Nakamura T, Ohishi K, et al. Active production of anti-human T-lymphotropic virus type I (HTLV-I) IgM antibody in HTLV-I–associated myelopathy. J Neuroimmunol 1991;32:105–9
33. Moritoyo T, Reinhart TA, Moritoyo H, et al. Human T-lymphotropic virus type I–associated myelopathy and tax gene expression in $CD4^+$ T lymphocytes. Ann Neurol 1996;40:84–90
34. Matsuoka E, Takenouchi N, Hashimoto K, et al. Perivascular T cells are infected with HTLV-I in the spinal cord lesions with HTLV-I–associated myelopathy/tropical spastic paraparesis: Double staining of immunohistochemistry and polymerase chain reaction in situ hybridization. Acta Neuropathol 1998;96:340–46
35. Seki M, Higashiyama Y, Mizokami A, et al. Up-regulation of human T lymphotropic virus type 1 (HTLV-1) tax/rex mRNA in infected lung tissues. Clin Exp Immunol 2000;120:488–98